

Fig. S1. (a) bright- and (b) dark field high resolution TEM images of $\text{WO}_3\text{-8Ti}$.

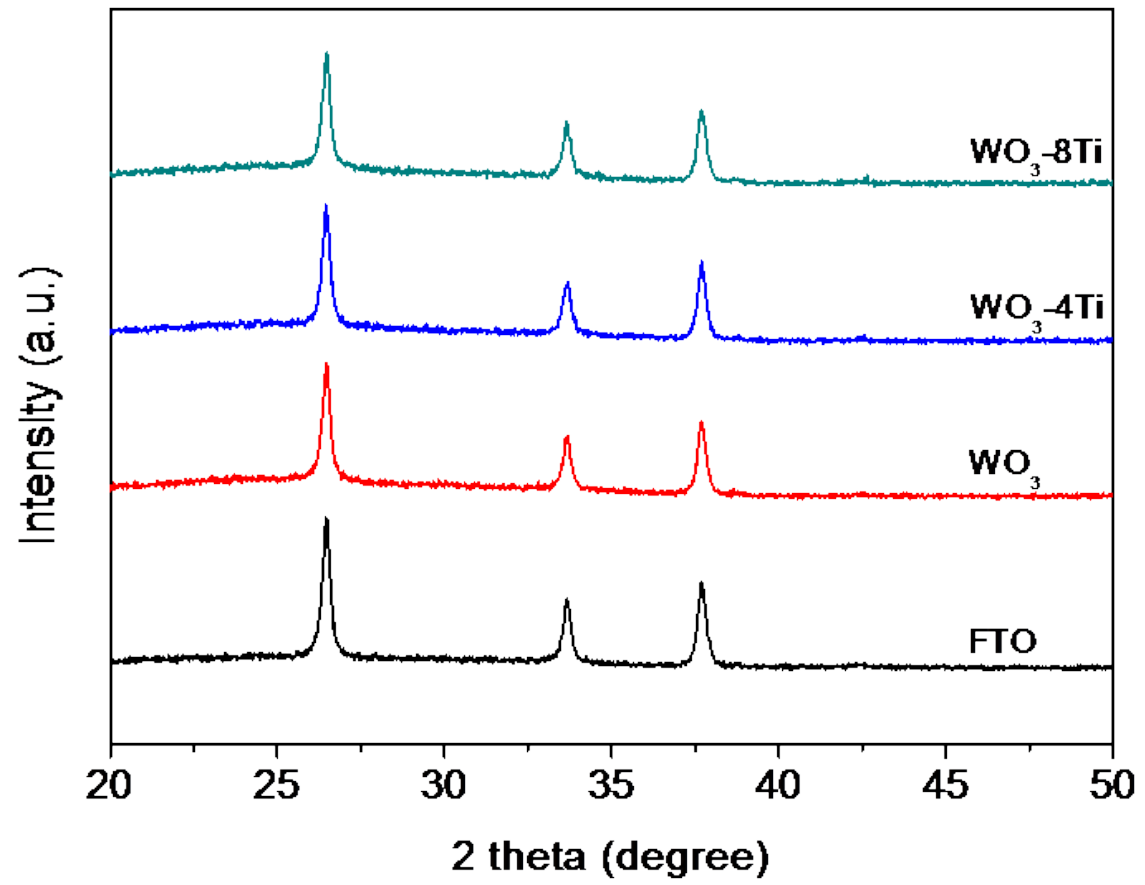


Fig. S2. XRD patterns of FTO/glass, WO₃, WO₃-4Ti and WO₃-8Ti, respectively.

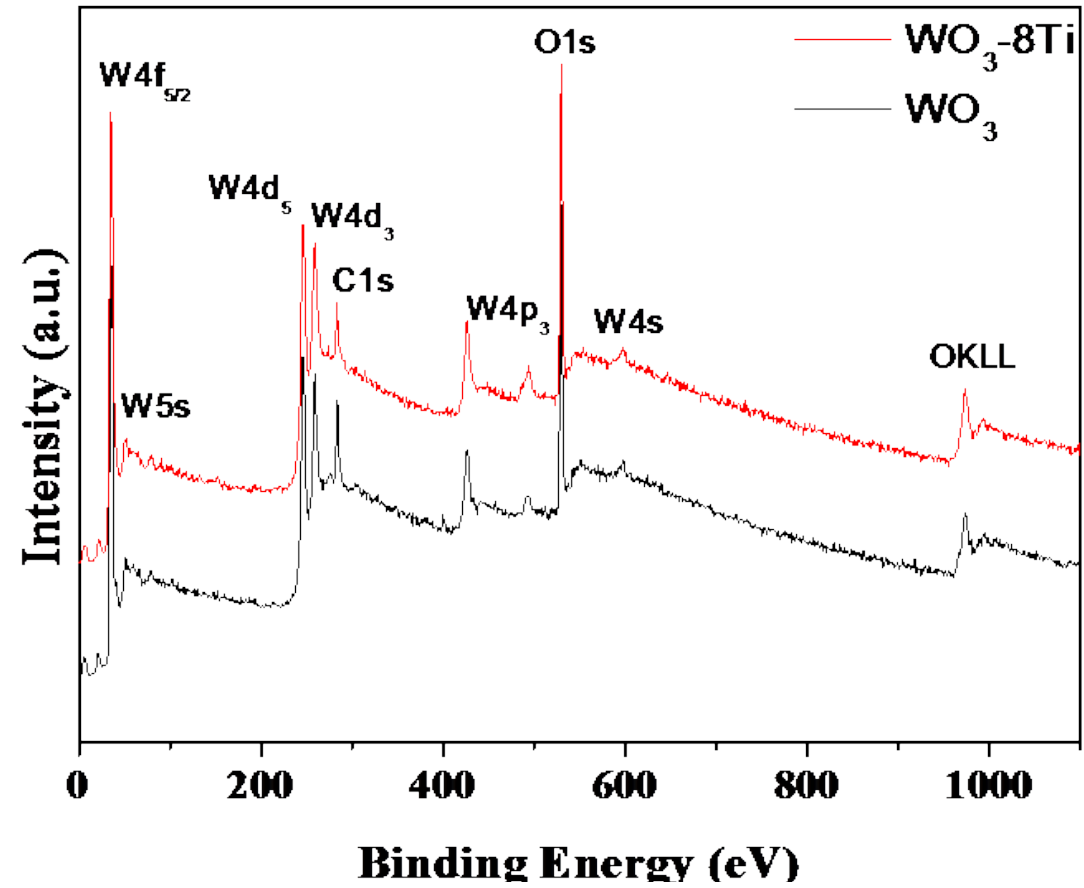


Fig. S3. XPS survey spectra of WO_3 and $\text{WO}_3\text{-8Ti}$, respectively.

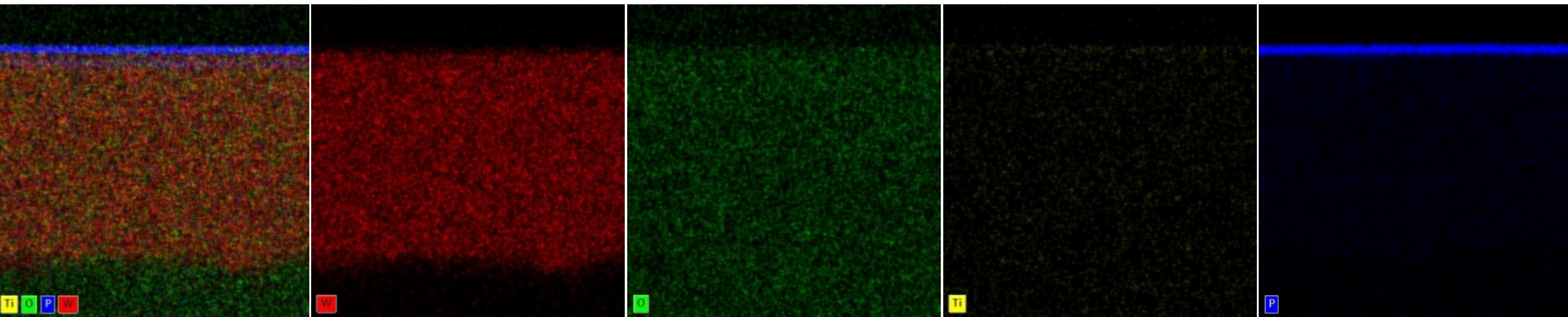


Fig. S4. EDS maps of $\text{WO}_3\text{-8Ti}$.

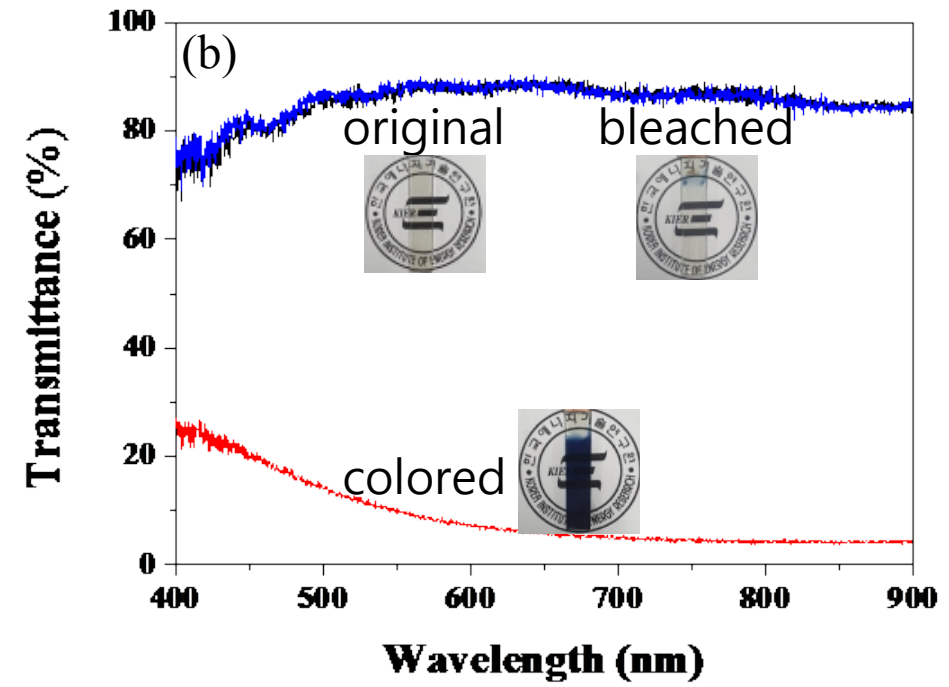
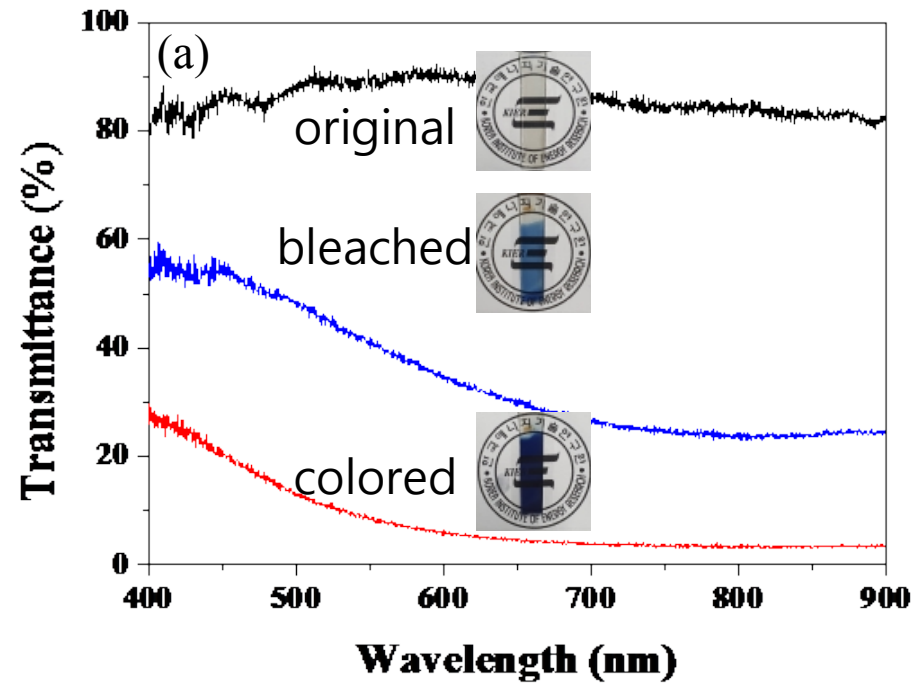


Fig. S5. In situ optical response of (a) neat WO_3 and (b) $\text{WO}_3\text{-8Ti}$ at 10th CA cycle. Inset shows the photo images at original, colored and bleached state of WO_3 films, respectively.

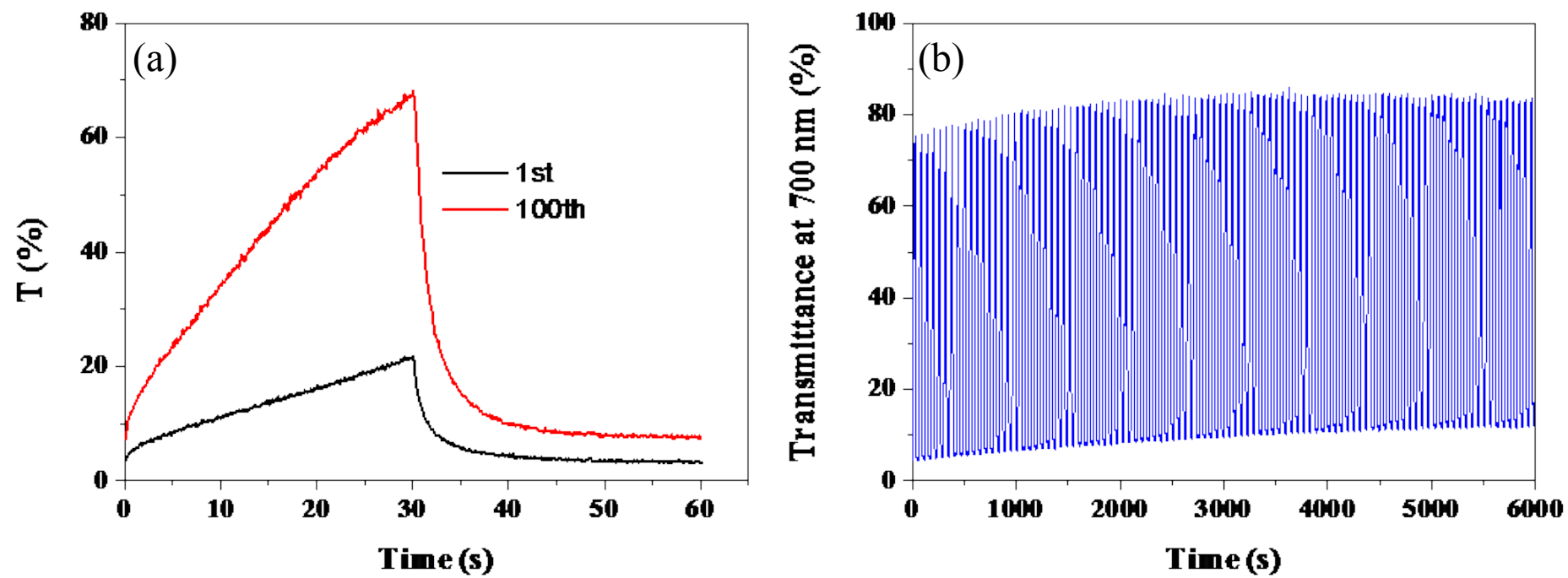


Fig. S6. (a) 1st and 100th switching curves of WO_3 films (b) Cycle performance of the WO_3 -4Ti film measured in 1.0 M LiClO_4 for 6000 s.

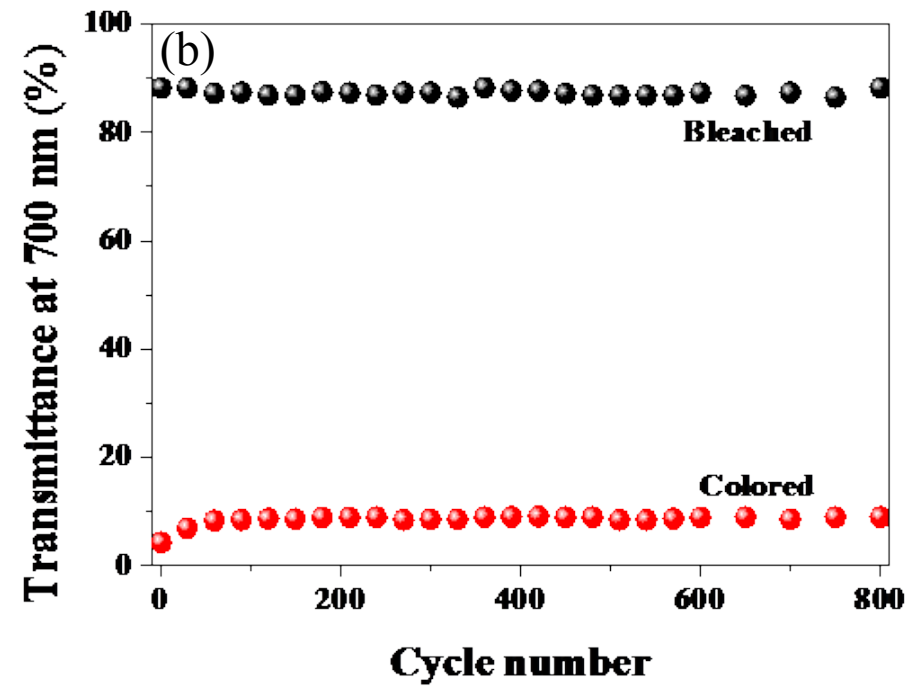
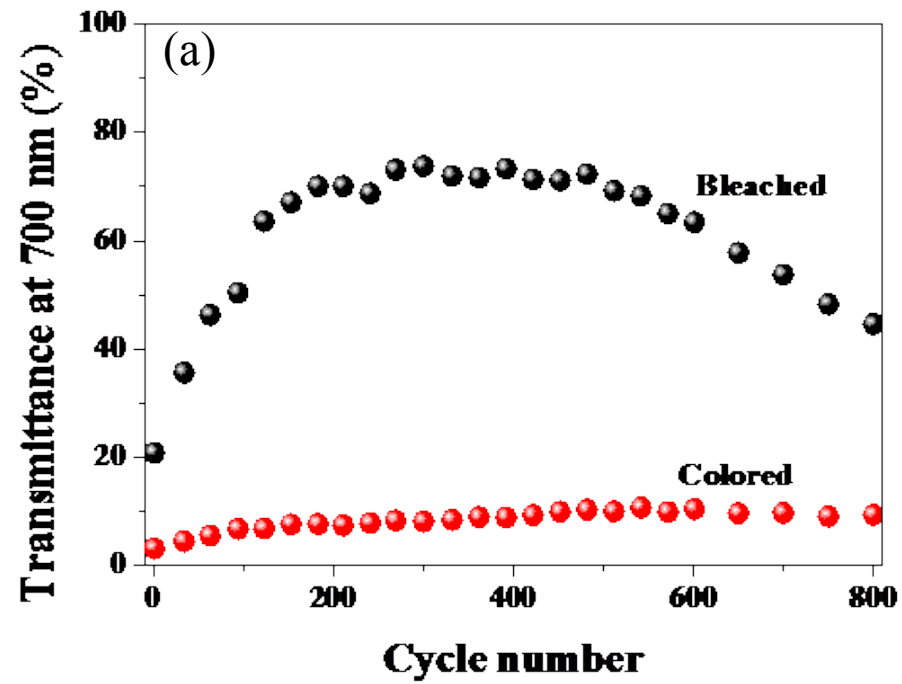


Fig. S7. *In situ* optical transmittance of (a) neat WO_3 and (b) WO_3 -8Ti at 700 nm.

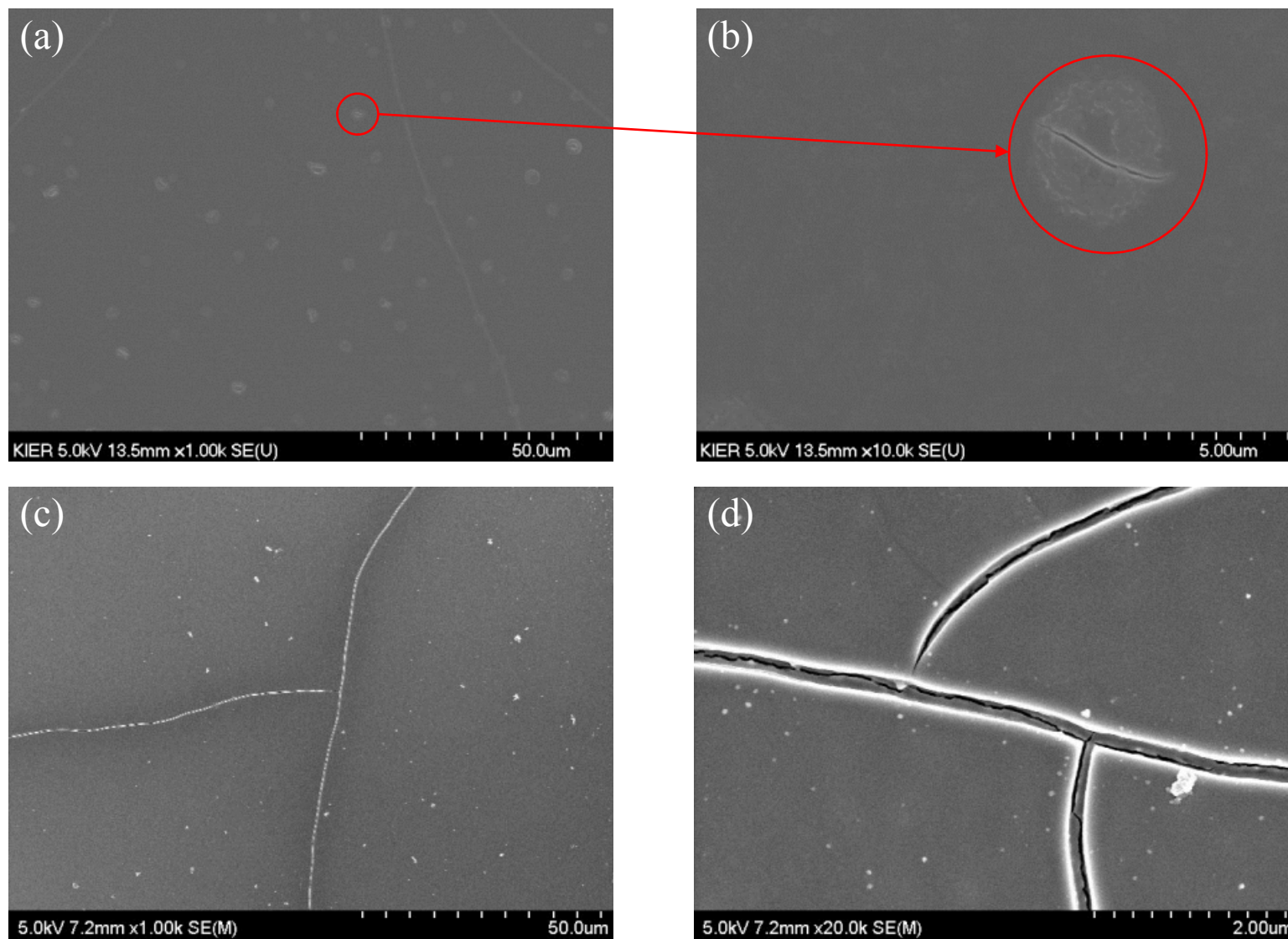


Fig. S8. (a-b) SEM image of the neat WO₃ film after 100th and 800th cycle. (c-d) Enlarged view of (a) and (b).